ARTICLE

The analysis of saltwater intrusion through Komesu underground dam and water quality management for salinity

Norio Nawa · Kenji Miyazaki

Abstract The Komesu underground dam is the first full-scale underground dam constructed to prevent saltwater intrusion in Japan. Although the cutoff wall of the dam effectively reduces the movement of saltwater into the reservoir area, saltwater masses remained behind the dam at the time of its completion, and saltwater can intrude beneath and diffuse through the wall, particularly when the reservoir level is below the sea level because of high pumping levels during the drought years. Therefore, it is necessary to estimate in advance whether the saltwater concentration in the pumped water is likely to exceed or not the permissible salinity level because of an increase in the residual saltwater mass as a result of saltwater intrusion and to take necessary measures to suitably manage the saltwater level behind the dam. To analyze saltwater intrusion, we first selected the optimal program suitable for the analysis of saltwater intrusion. Second, we examined the longitudinal dispersivity and the effect of the cone of depression around the pumping wells. Then we analyzed saltwater intrusion into the reservoir area in detail by using a two-dimensional convective–dispersive analysis. The results of the analysis make it possible to improve management of saltwater in the reservoir area behind the underground dam.

N. Nawa (✉)
National Irrigation Project Office of the Waga Middle Area
District, Tohoku Regional Agricultural Administration Bureau,
Ministry of Agriculture, Forestry and Fisheries,
6-131-1 Naganuma, Wagamachi, Kitakami,
Iwate 024-0333, Japan
e-mail: kpncf647@ybb.ne.jp

K. Miyazaki
Sanyu Consultants Inc., 2-15-22 Nishiki, Nakaku, Nagoya,
Aichi 460-0003, Japan

Introduction

The National Irrigation Project of the Okinawa Main Island Southern Area District (NIPOOMISAD 2006) was carried out in a field with an area of 1,352 ha, where vegetables, leaf tobacco and mainly sugarcane were grown from 1992 to 2005. The purpose of the project was to develop agriculture in the district by securing a stable supply of water for agriculture, improve agricultural productivity and product quality, and stabilize farming management.

This project comprised two underground dams, six pumping stations and 42 km of irrigation pipelines (Fig. 1). The Komesu underground dam, which consists of a cutoff wall and reservoir area, is the main water source for the project. It was constructed along the coastal area in Itoman city, Okinawa, Japan. The cutoff wall extends for 2,320 m; its deepest point is −69.4 m, and the reservoir capacity is about 3.5 million m^3. The low water level of the reservoir is −11.6 m, relative to the sea level. This dam is the first full-scale underground dam, designed to prevent saltwater intrusion, which has ever been built in Japan. The cutoff wall is a continuous wall made of concrete with a thickness of more than 54 cm (Fig. 2). Eighteen pumping wells, with a maximum average daily pumping capacity of 2,000 m^3, were drilled in the reservoir area (Fig. 3).
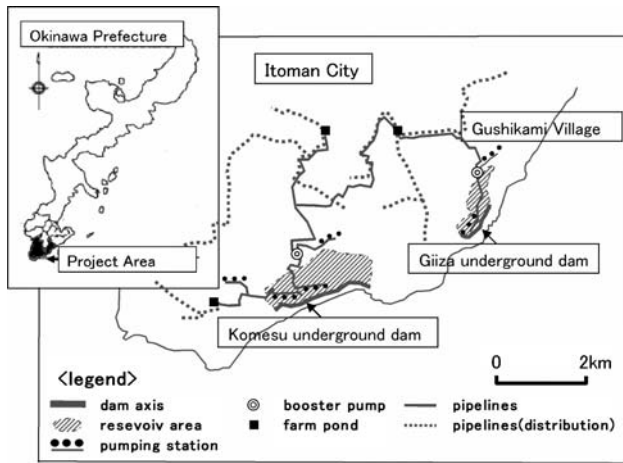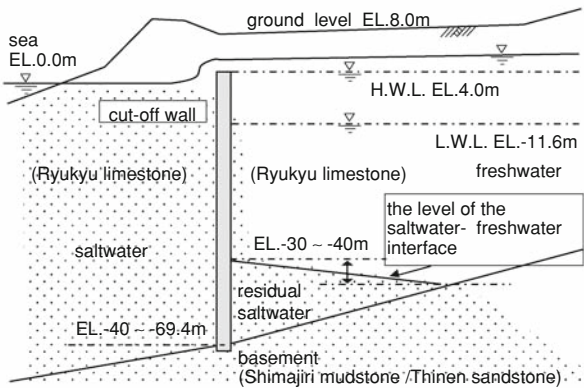
The permissible salinity level for agriculture, expressed as the concentration of chlorine, established by this project is 200 mg/l, which is the highest permissible salinity for the least chlorine-resistant cultivar of string beans

Fig. 1 Implementation map of the National Irrigation Project of the Okinawa Main Island Southern Area District

Fig. 2 Outline of Komesu underground dam

among the regionally grown crops. This permissible chlorine concentration is the same as that for potable water.

During the construction of the underground dam, the cutoff wall was gradually constructed outwards, starting from the center to the sides of the reservoir, to allow

natural drainage of as much residual saltwater from the reservoir as possible. Nevertheless, residual saltwater masses remained in depressions near the eastern and western ends of the dam after its completion (Fig. 3). Vertical profiles of electrical conductivity (EC) values in observation wells in the western part of the reservoir are shown in Fig. 4. EC increases slightly with depth to around 5,000 μS/cm (chlorine concentration, 1,500 mg/l), when the increase becomes large. The exact location of the interface between freshwater and freshwater–saltwater mixing, however, is not clear. We therefore estimated the EC of the residual saltwater masses to be more than 5,000 μS/cm and arbitrarily defined the water level at which the EC reached 5,000 μS/cm as the saltwater–freshwater interface, including the freshwater–saltwater mixing zone. The present level of this interface is at −30.0 m at the western end and −40.0 m at the eastern end of the dam. When the groundwater level in the reservoir is below sea level, it is possible for new saltwater to intrude through the cutoff wall and beneath its foundation, thus increasing the volume of the residual saltwater mass in the reservoir and allowing the saltwater to be drawn toward the pumping wells. Therefore, it is desirable to estimate in advance whether the salinity of the pumped water that is being used for irrigation is likely to exceed or not the permissible level and to take necessary measures to prevent such exceeding by proper management of the reservoir.

Water tank experiment and comparison of analysis programs

Many numerical and experimental studies of saltwater intrusion have been conducted, but the movement of residual saltwater in a reservoir above a sloping basement has been scarcely considered (Henry 1959; Momii et al. 1989; Boufadel et al. 1999; (Nawa et al. 2008). Therefore, we first studied the movement of residual saltwater in a

Fig. 3 Position of dam axis, pumping wells and residual saltwater areas in Komesu underground dam
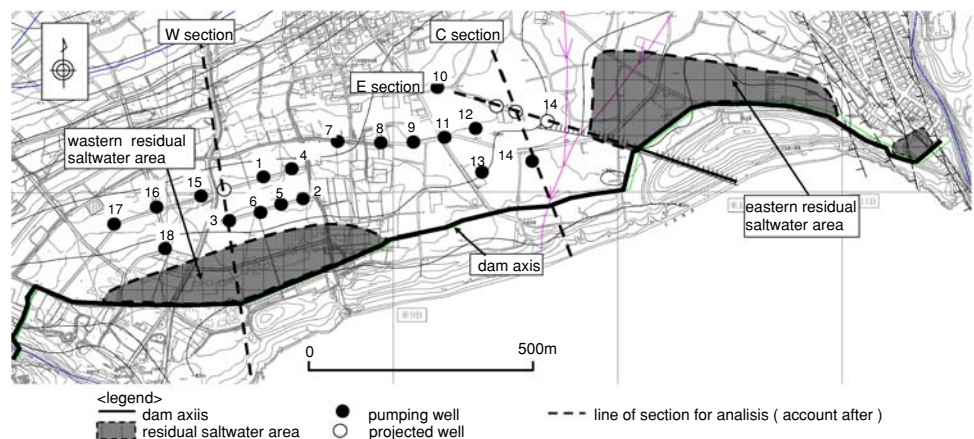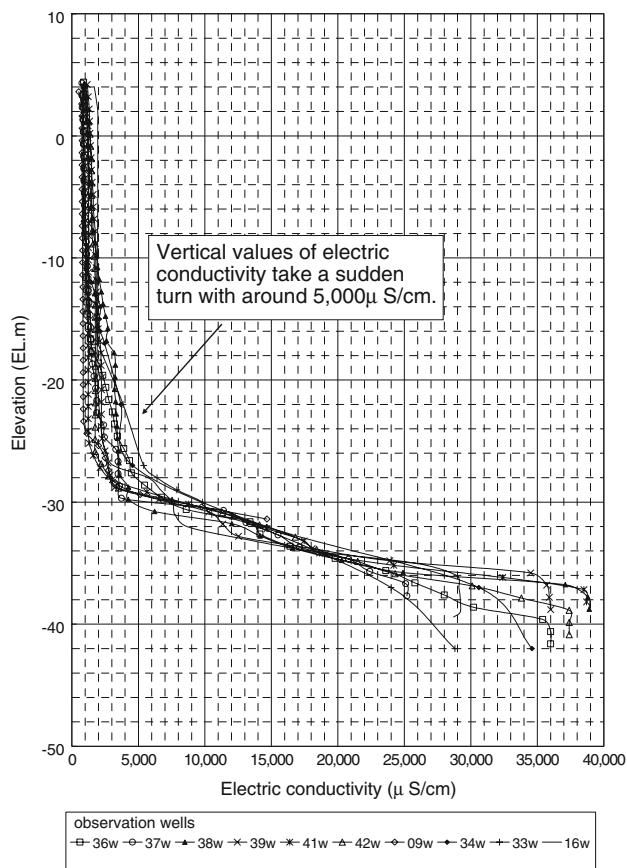
Fig. 4 Vertical profiles of electric conductivity values in observation wells in the western residual saltwater area

water tank experiment (Fig. 5). We used the data obtained in the experiment as data for validation of our saltwater intrusion model.

Numerical calculation of saltwater intrusion is dependent on the convective–dispersive equation. It is given as follows (Nishigaki et al. 1995):
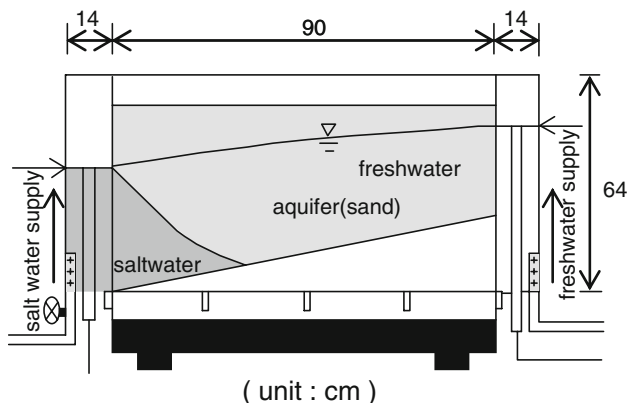
Fig. 5 Outline of water tank experiment

$$\theta\rho\frac{\partial c}{\partial t} = \frac{\partial}{\partial x_i}\left(\theta\rho D_{ij}\frac{\partial c}{\partial x_j}\right) - \frac{\partial}{\partial x_i}(\theta\rho V_i c) \tag{1}$$

$$D_{ij} = \alpha_{\mathrm{T}}\|V\|\delta_{ij} + (\alpha_{\mathrm{L}} + \alpha_{\mathrm{T}})\frac{V_i V_j}{\|V\|} + \tau\delta_{ij} \tag{2}$$

where, on the right side of Eq. 1, the first term is the dispersive term and the second term is the convective term, c is the concentration, t is time, θ is volumetric fluid content, ρ is density of fluid, x is coordinate, D_{ij} is dispersivity tensor, where subscripts i and j stand for x_i, x_j, respectively, x_i, x_j are Cartesian coordinates, V_i is velocity vector of fluid, α_{T} is transversal dispersivity, α_{L} is longitudinal dispersivity, $\|V\|$ is norm of velocity, τ is tortuosity, and δ_{ij} is Kronecker delta.

The convective term of the equation affects computational stability, so its objective applicability and calculation accuracy depend on the discretization procedure used by the software to implement the analysis. Therefore, we selected the optimal program suitable for analysis of saltwater intrusion though this underground dam after a comparative review of programs and of the applicability of the discretization procedure used by each program for the convective term.

The final candidates were DTRANSU (Nishigaki et al. 2001), SEAWAT (Guo and Langevin 2002) and SUTRA (Voss and Provost 2003). These programs all permit two- or three-dimensional density-dependent flow analysis, and their source codes and analytical approaches are available.

Though one- and two-dimensional flow analyses by the three programs were compared, a two-dimensional residual saltwater movement analysis on inclined ground, recreating the movement of residual saltwater in the water tank experiment, was made. The mesh is divided into 1 cm in both horizontal and vertical directions on the basis of a longitudinal dispersivity of 0.07 cm. The other parameter values used in the calculation are hydraulic conductivities $k_1 = 0.2$ cm/s in the horizontal direction, $k_2 = 0.1$ cm/s in the vertical direction, storage coefficient $S = 0.49$, longitudinal dispersivity $\alpha_{\mathrm{L}} = 0.07$ cm, transversal dispersivity $\alpha_{\mathrm{T}} = 0.007$ cm, density of freshwater $\rho_{\mathrm{f}} = 1.000$ g/cm^3 and density of saltwater $\rho_{\mathrm{s}} = 1.023$ g/cm^3. The hydraulic conductivities k_i and storage coefficient S are used to calculate seepage movement of flow. Figure 6 shows the stability solutions of SEAWAT, using the MOC (method of characteristics) or MMOC (modified method of characteristics) discretization procedure, of DTRANSU using MMOC and of SUTRA using upstream weighting to discretize the convective term. EC1 and EC2 in Fig. 6 are the observation points of EC in the water tank experiment. Dimensionless concentrations of EC1 and EC2 at the time of carrying out the water tank experiment are 0.5 at each
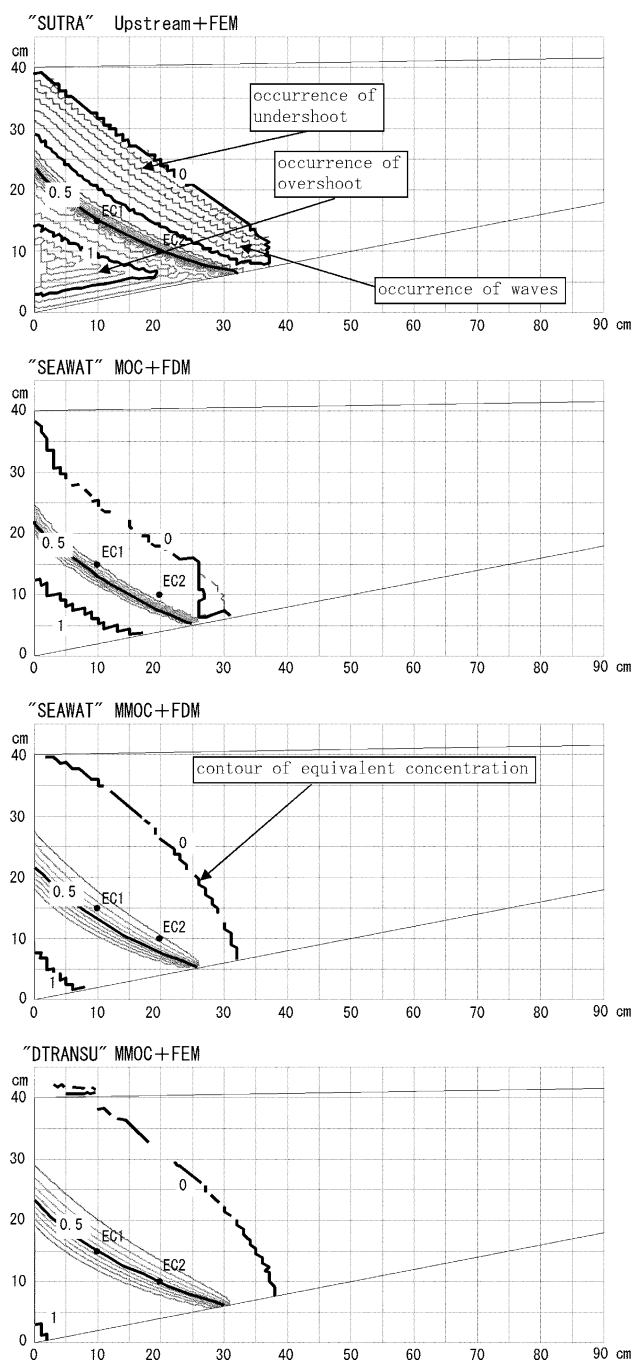
Fig. 6 Simulated concentration by the two-dimensional residual saltwater movement analysis in the water tank experiment. Note: The equivalent lines of dimensionless concentration are drawn by 0.1. EC1 and EC2 are the observation points of EC in the water tank experiment

other. These observed values are used in the comparison of analysis programs. Figure 6 shows that both MOC and MMOC are suitable for discretization of the convective term in the analysis, which is applied on the different layer in dispersivity, because this inhibits the generation of the dispersion of calculation and the outlier detection.

Although SEAWAT(MMOC + FDM) and DTRAN-SU(MMOC + FEM) are suitable for the analysis program, DTRANSU, which discretizes the dispersive term in the convective–dispersive equation by FEM, is suitable to reflect the situations of the analysis object by using the finite element mesh and was selected as the analysis program [i.e., FDM (finite difference method), FEM (finite-element method)].

Field survey of longitudinal dispersivity

The longitudinal dispersivity parameter of the convective–dispersive equation must be determined before the analysis of saltwater intrusion can be carried out. We estimated this parameter by means of a tracer experiment. Although it is difficult to obtain a significant result in a field experiment, and successful results about limestone have not been obtained in Japan (SES 2002), we attempted a tracer experiment because the longitudinal parameter was basically obtained in the field.

Flow field

In a tracer experiment, a concentration–time curve is drawn that shows changes in the concentration of a tracer injected into the groundwater flow as measured at an observation well. This curve is then compared with a concentration–time curve obtained by approximation analysis to estimate the longitudinal dispersivity. The analysis assumes a parallel or radial flow field. Therefore, we assumed a converging radial flow toward a pumping well and injected the tracer into a nearby well. The tracer concentration was observed in the pumping well.

Experimental setup

Existing pumping wells (φ400 mm) and observation wells (φ50 mm) were used in the experiment. The distance between the tracer injection well and the pumping well where the concentration was measured ranged from 8 to 53 m, and the reservoir thickness from 25 to 30 m. The average hydraulic conductivity of the pumping well estimated by a pumping test ranged from 10^{-1} to 10^{0} cm/s. The slope of the cone of depression around the pumping well was small, and its depth ranged from 1 to 8% of the thickness of the reservoir.

Results of the experiment

The longitudinal dispersivity was estimated by comparing the measured concentration–time curve with standard curves derived from the equation of Sauty (Sauty 1989; SGGP 1991). The equation is given as follows:

$$c_R = \frac{K_R}{t_R^{1.5}} \exp\left(-\frac{P_e}{4t_R}(1-t_R)^2\right) \qquad (3)$$

$$P_e = \frac{r}{\alpha_L} \qquad (4)$$

$$K_R = t_{R\max}^{1.5} \exp\left(\frac{P_e}{4t_{R\max}}(1-t_{R\max})^2\right) \qquad (5)$$

$$t_{R\max} = \left(1 + 9P_e^{-2}\right)^{1/2} - 3P_e^{-1} \qquad (6)$$

where c_R is $c/c_{\max}$ with $c_{\max}$ peak concentration at the time of peak concentration $t_{R\max}$, t_R is $t/t_{R\max}$, P_e is Peclet numbers, r is the distance between the tracer injection well and the pumping well, and α_L is the longitudinal dispersivity.

We conducted the experiment at four pumping wells and obtained as a result seven concentration–time curves (Fig. 7). The concentration–time curves were not all clear peak curves similar to the standard curves; some were bimodal curves with a stepped pattern, such as those obtained at wells No. 1 (8 m) (i.e., the No. 1 well is the pumping well and the observation well of tracer concentration and 10 m is the distance between the No. 1 well and tracer inject well) and No. 5 (10 m). The concentration in well No. 5 (10 m) and No. 9 (36 m) decreased very slowly after the concentration peak. In addition, the peak concentration in the No. 9 well (53 m) appeared earlier than that in the No. 9 well (36 m). A staircase pattern implies that the tracer passed through layers with different properties, and a very slow reduction in the tracer concentration after the peak implies that the tracer followed various paths, each with a different travel time.

Comparisons with the standard curves are shown in Fig. 8. The observed curves and the standard curves do not completely coincide. In addition, the estimated
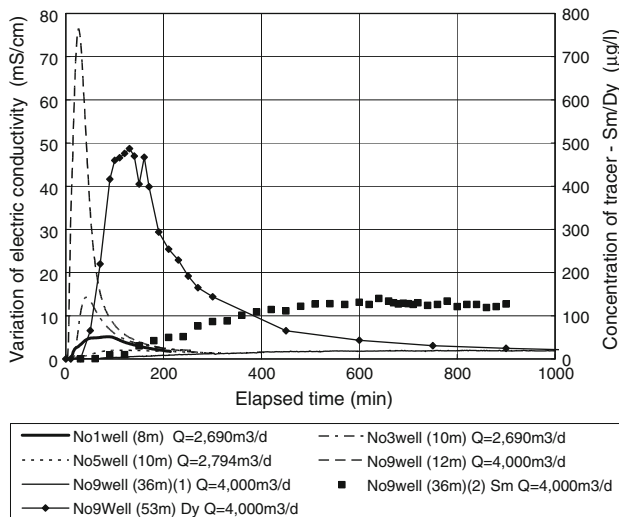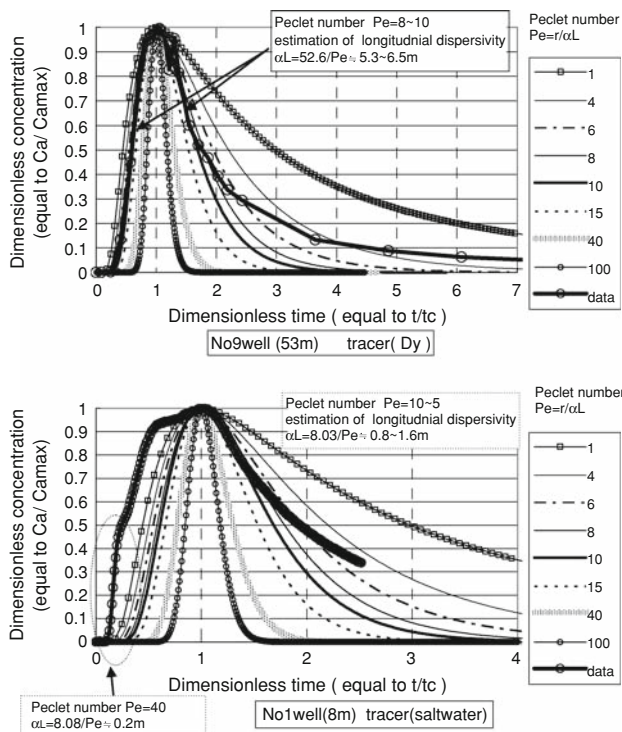

Fig. 8 Estimation of longitudinal dispersivity by comparisons of observed curves and standard curves for analysis

longitudinal dispersivity differed depending on how the observed peak was identified and whether its position was determined to be before or after the peak of the standard curve. The estimated longitudinal dispersivities about the peaks of all curves ranged from 0.8 to 6.5 m, with most values ranging from 1 to 2 m or around 5 m. The longitudinal dispersivity in the most pervious layer was estimated to be 0.2–0.5 m. The results for the No. 9 well (36 m) and No. 5 well (10 m), where the concentration decreased very slowly, fall beyond the range of application of the standard curve, and the longitudinal dispersivity apparently became very large over the experimental distance. The estimated longitudinal dispersivity is consistent with the relationship between the observation scale and the longitudinal dispersivity in the experimental data (SES 2002). Therefore, we used a longitudinal dispersivity of 5 m around pumping wells of the Komesu groundwater dam in our analysis.

Analysis of saltwater intrusion

Two-dimensional analysis model

Saltwater intrusion was analyzed in four sections, using a two-dimensional vertical-section analysis model. Here, we discuss the results of three representative sections (Fig. 3).

Fig. 7 Observed concentration–time curves by the tracer experiment

The western (W) and eastern (E) sections were near the residual saltwater masses, where the movement of residual and intruding saltwater to the pumping wells was anticipated. These sections were used to estimate whether and how much saltwater removal was needed. The movement of the eastern residual saltwater mass to well No. 14 was also estimated for section E by projecting the location of the well onto the section, which was drawn perpendicular to the direction of the cutoff wall.

The central (C) section, which did not pass through a residual saltwater mass, was drawn through the center of the dam axis. The movement of intruding saltwater from near the cutoff wall to the pumping wells was estimated in section C.

The geological conditions of each section are shown in Fig. 9. The hydraulic coefficients (Table 1) used in the calculations were from available field experiment results (NIPOOMISAD 2006).

The year covered by the calculations was the design reference year 1971. The calculation period was from 1 May to 31 December, when the reservoir level was lower than the crest of the dam. The calculation results of a water balance model were adopted for the amount of water pumped from the pumping wells, rainfall-induced groundwater recharge and groundwater flow from upstream sites. The initial proxy for salinity was estimated by a simulation in which the initial values were set by referring to observed salinity (as the chlorine concentration) results.

Saltwater movement in the reservoir

The results of the saltwater intrusion analysis in the W and E sections, which pass through the residual saltwater mass, showed that the movements of the residual and intruding saltwater differed according to the reservoir level (Fig. 10).

Reservoir level and saltwater movement

(1) Reservoir level more than 4.0 m (overflow over the top of the cutoff wall, no saltwater intrusion)
The groundwater level in the reservoir is over the crest of the cutoff wall, and overflow occurs. The residual saltwater in the reservoir is pushed toward the wall, and the zone of freshwater–saltwater mixing rises up around the cutoff wall and a little flows over the top. As the water level increases as a result of rainfall, the residual saltwater is pushed more strongly against the cutoff wall. This situation was confirmed by field measurements. Some saltwater also diffuses out of the reservoir through the cutoff wall and below its foundation.

Fig. 9 Geology of two-dimensional section models
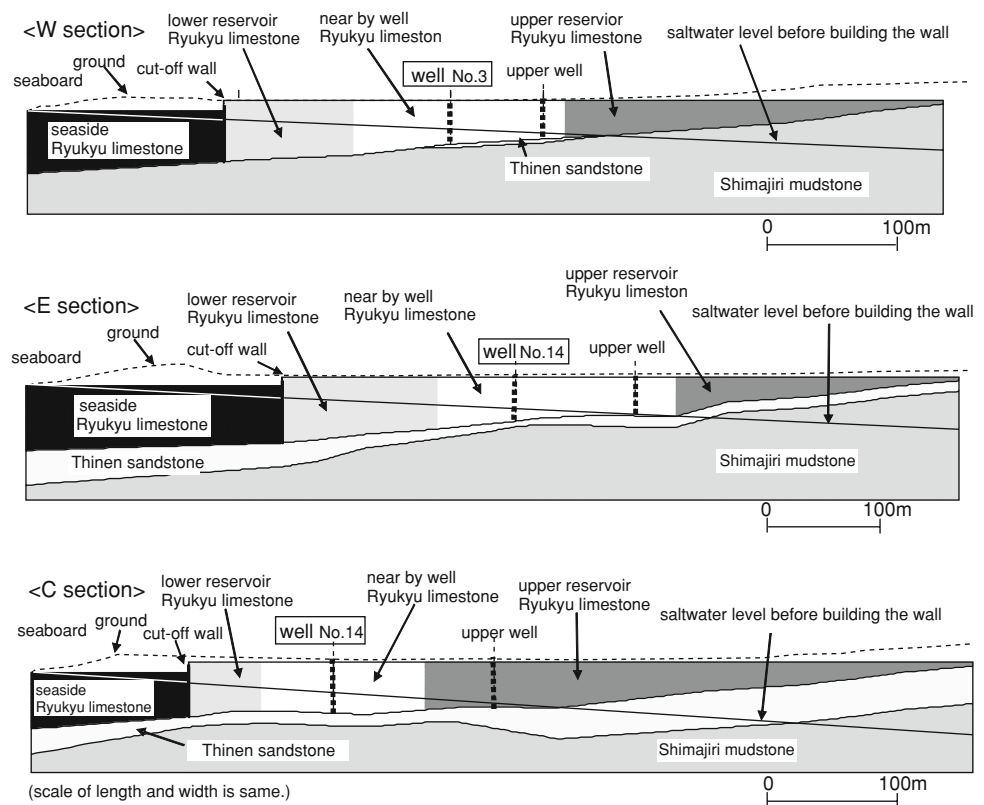
Table 1 Hydraulic coefficients of two-dimensional section models

Area	Matter		W plane	C plane	E plane
All	Density of liquid (g/cm³)	Freshwater	1.002 (relative density 1.000)		
		Saltwater	1.025 (relative density 1.023)		
Ryukyu limestone	Hydraulic conductivity k(cm/s)	Seaside	8.4×10^{-1}	8.4×10^{-1}	8.4×10^{-1}
		Lower reservoir	8.4×10^{-1}	3.3×10^{-2}	8.4×10^{-1}
		Near by well	8.4×10^{-1}	3.3×10^{-2}	3.3×10^{-1}
		Upper reservoir	8.4×10^{-1}	8.4×10^{-1}	8.4×10^{-1}
	Storage coefficient S	Seaside	0.094	0.094	0.094
		Lower reservoir	0.094	0.04	0.094
		Near by well	0.094	0.04	0.04
		Upper reservoir	0.094	0.094	0.094
	Longitudinal despersivity α_L (m)	Seaside	1.0	1.0	1.0
		Lower reservoir	1.0	1.0	1.0
		Near by well	5.0	5.0	5.0
		Upper reservoir	1.0	1.0	1.0
Thinen sandstone	k(cm/s)		2.0×10^{-5}	2.0×10^{-5}	2.0×10^{-5}
	S		0.03	0.03	0.03
	α_L(m)		0.001	0.001	0.001
Shimajiri mudstone	k(cm/s)		5.0×10^{-6}	5.0×10^{-6}	5.0×10^{-6}
	S		0.03	0.03	0.03
	α_L(m)		0.001	0.001	0.001
Cutoff wall	Thickness t(m)		0.54	0.54	0.54
	k(cm/s)		6.0×10^{-7}	6.0×10^{-7}	6.0×10^{-7}
	S		0.03	0.03	0.03
	α_L(m)		0.001	0.001	0.001

Transversal dispersivity is 1/10 of longitudinal dispersivity

(2) Reservoir level 4.0–1.5 m (no overflow, no saltwater intrusion)

The groundwater level in the reservoir is lower than the crest of the dam, so no overflow occurs, but no saltwater intrudes because the water level in the reservoir is still much higher than sea level. Some saltwater diffuses through the cutoff wall and below its foundation. The residual saltwater that was pushed toward the cutoff wall during overflow returns toward the middle of the reservoir, and the water level in the reservoir, and the level of the saltwater–freshwater interface, flattens. The amount of saltwater in the reservoir does not increase.

(3) Reservoir level 1.5–0.0 m (no overflow, partial saltwater intrusion)

Along section E, when the groundwater level in the reservoir falls to about 1.5 m, saltwater begins to intrude into the reservoir near the bottom of the cutoff wall (−65 m). Similarly, along the W section, when the groundwater level is about 1.0 m, saltwater begins to intrude into the reservoir near the bottom of the cutoff wall (−40 m). The intrusion part and the no intrusion part of saltwater are mixed according to the depth of the cutoff wall.

(4) Reservoir level less than 0.0 (no overflow, saltwater intrusion)

Saltwater intrudes through the entire cutoff wall and below its foundation and the amount of saltwater in the reservoir increases. The intruding saltwater moves to the bottom owing to its greater density and mixes with the residual saltwater. Therefore, the amount of saltwater increases gradually and the level of the saltwater–freshwater interface increases. Close to pumping wells, the saltwater is drawn upward along the basement surface.

Movement of saltwater by water pumping

When groundwater is pumped, its surface forms a cone of depression around each pumping well. If there is saltwater in the region of the drawdown, the saltwater moves toward
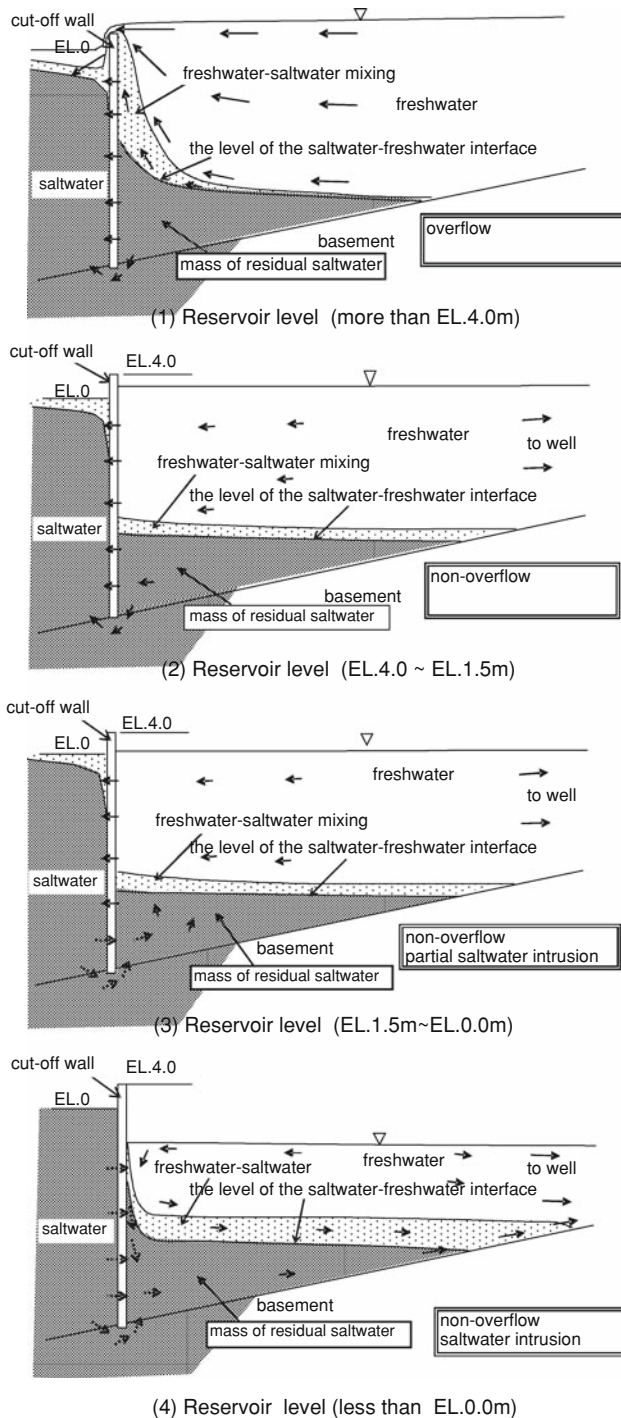
Fig. 10 Conception of reservoir level and saltwater movement in the reservoir area

the well. Though mixed freshwater–saltwater generally arrives at the well eventually, the denser saltwater usually does not reach the well because of the gradual groundwater surface slope and the steep slope of the basement approaching the well. How much saltwater arrives at the well depends on the distance between the well and the

saltwater mass, the degree of drawdown by water pumping, the density of the saltwater, and the basement slope.

Variation of flow velocity in relation to drawdown around the pumping wells

The pumping wells are arranged in a line roughly parallel to the cutoff wall. Therefore, the groundwater flow to the wells during pumping can be characterized as a parallel flow in a direction perpendicular to the cutoff wall far from the wells, but close to each well the flow is radial (Fig. 11). In a two-dimensional analysis, however, the radial flow near the well is expressed as parallel flow, and the flow velocity does not increase as a result of the drawdown near the pumping wells (Fig. 11). Thus, the saltwater arrival time calculated in a two-dimensional analysis is later than the actual arrival time, and the estimated salinity of the pumped water is lower than the actual salinity. To quantify these differences, we constructed a two-dimensional cross-section model in which the X axis is half the distance between the wells and the Y axis is the distance between the cutoff wall and a well. In the analysis, the difference in the saltwater arrival time between parallel flow and radial flow was simulated with hydraulic coefficients that depended on the geological condition and the average amount of water pumped (Fig. 12). The dimensionless salinity, relative to salinity of seawater, at the pumping well ranges from 0.01 to 0.1; these densities range from 1.0002 to 1.0023. Vertical movement dependent on density is ignored because these densities (1.0002–1.0023) are mostly invariable in the density (1.0000) of freshwater. Thus, the analysis model was changed from a three-dimensional model to a two-dimensional model.

The analysis results showed that with radial flow, the saltwater arrival at the pumping well was about 0.5 day earlier than that with parallel flow. Therefore, an extra day in which the salinity of the pumped water is the highest was simulated by calculating another 1 day in the two-dimensional model and the solved concentration is decided as the corrected value.
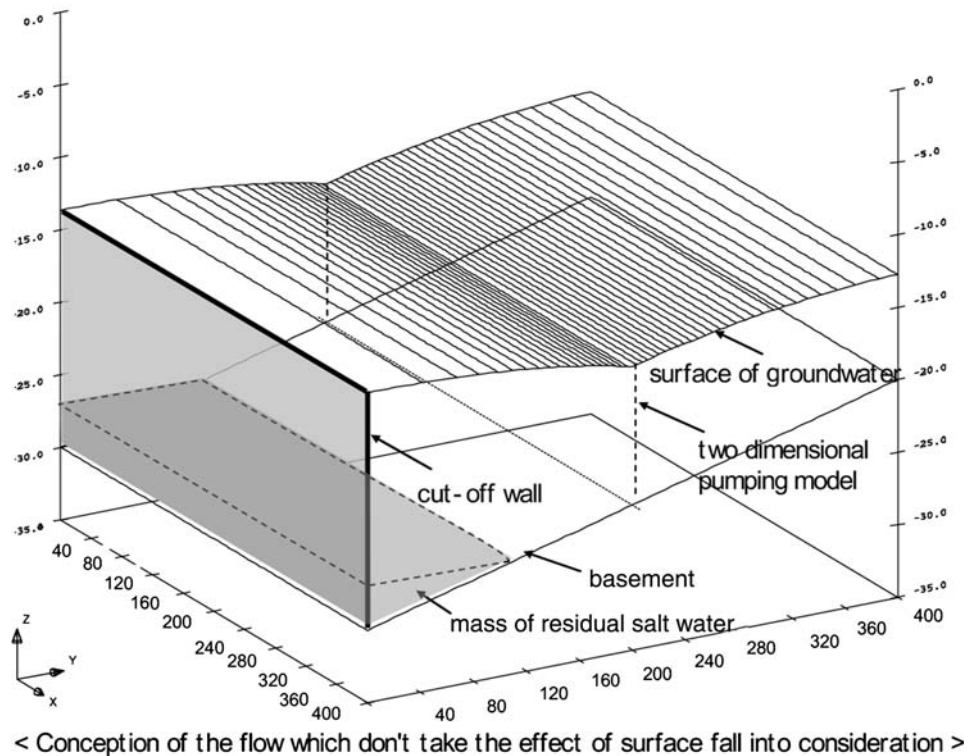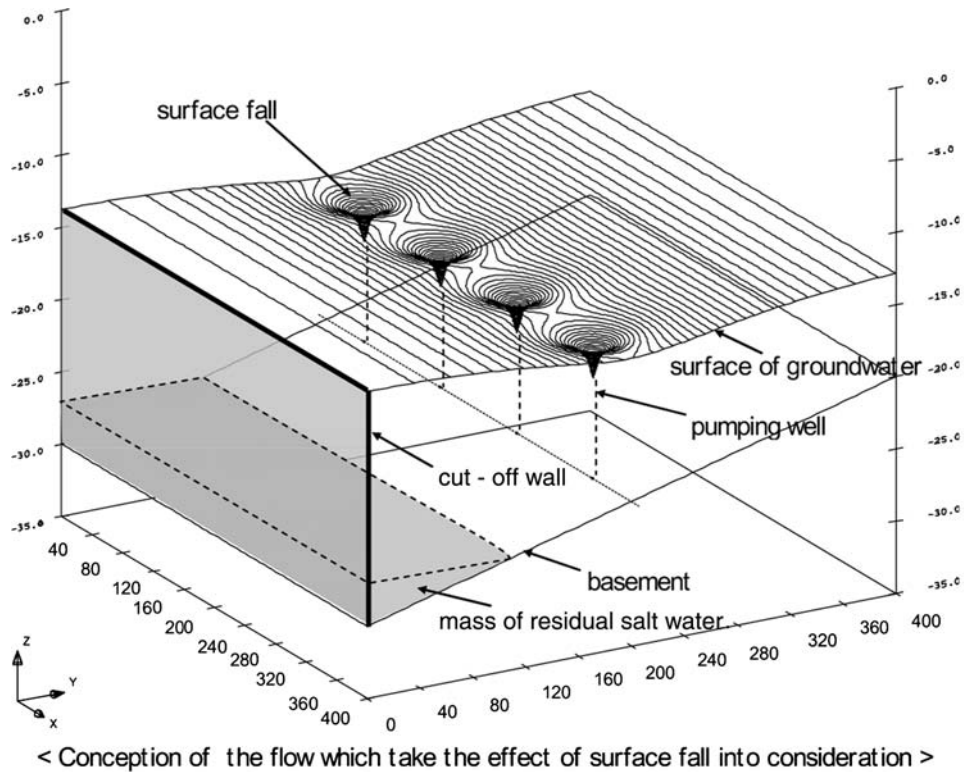
Influence on pumping wells of residual and intruded saltwater

Pumping wells near the residual saltwater mass

The well groups (E and W sections) near the residual saltwater masses were affected by both residual and intruded saltwater when water was pumped in the simulation based on the design reference year. The salinity (as the chlorine concentration) at both well No. 3 (W section) and well No. 14 (E section) was higher than the permissible salinity. Therefore,

Fig. 11 Conception of flow
around the pumping wells

< Conception of the flow which take the effect of surface fall into consideration >

< Conception of the flow which don't take the effect of surface fall into consideration >

another simulation was run in which the level of the salt-water–freshwater interface was reduced by the removal of saltwater (Fig. 13). When the level of the saltwater–freshwater interface was reduced to about −35 m in the W section

and about −43.5 m in the E section, the salinity of the pumped water becomes lower than the permissible salinity. This shows that the salinity of the pumped water in the design reference year would be lower than the permissible salinity if

Fig. 12 Velocity and concentration around the pumping well. Note: It is 20th after the start of calculation
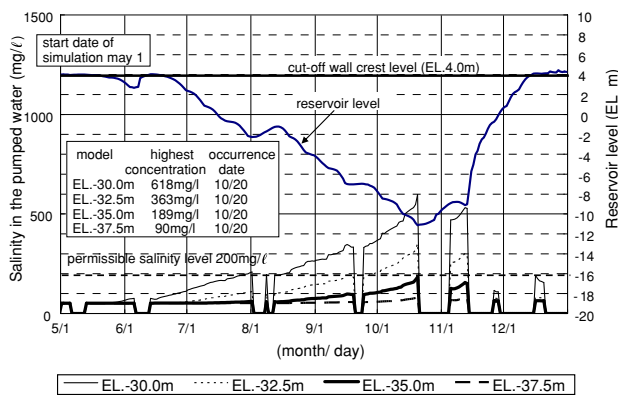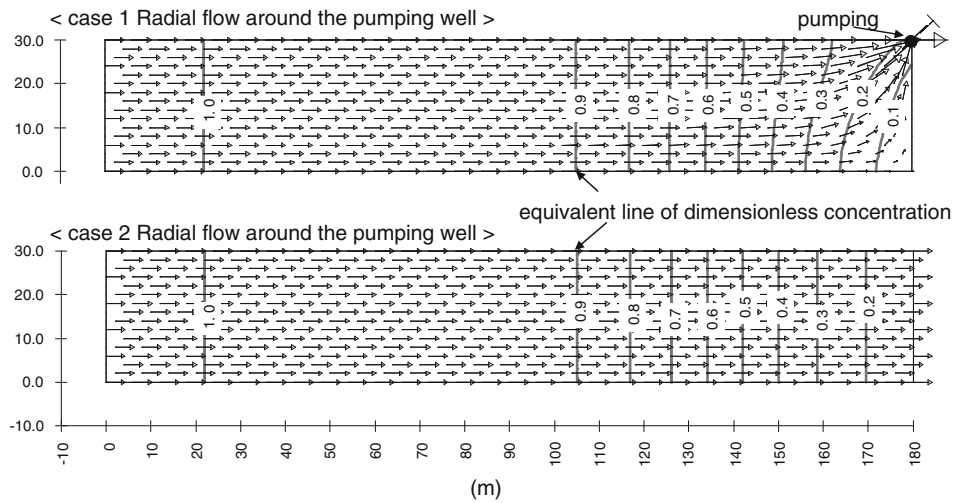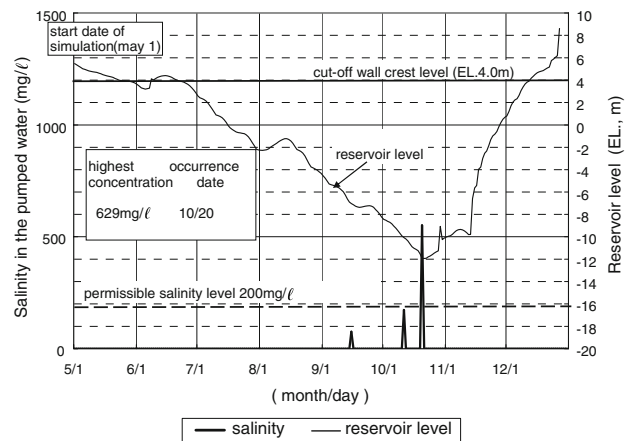

Fig. 13 Result of salinity in the pumped water by the saltwater intrusion analysis (W section, No. 3 well). Note, the elevations in the legend are the level of the saltwater–freshwater interface at simulation start point in time. When the salinity is 0, the driving of the pump stops

Fig. 14 Result of salinity in the pumped water by the saltwater intrusion analysis (C section, No. 14 well). Note: When the salinity is 0, the driving of the pump stops

saltwater is removed before every irrigation period to reduce the level of the saltwater–freshwater interface to those level (–35 m in the W, –43.5 m in the E). These levels can thus be considered as the target management levels of the saltwater–freshwater interface, and pumping should be performed until the interface is at these levels before every actual irrigation period. The difference in the amount of residual saltwater before pumping and the amount at the end of the design reference year is the amount of saltwater that needs to be removed.

Pumping wells near the cutoff wall

Well No. 14 is relatively near the cutoff wall in the central section (C section). In the simulation, the highest salinity was 629 mg/l, which exceeds the permissible salinity (Fig. 14). The pumped water from well No. 14 is mixed

with water pumped from six other wells in a farm pond, which had the highest predicted salinity of 66 mg/l.

Water quality management for salinity

Management facilities

The purpose of water quality management for salinity is to keep the salinity of irrigation water supplied from the reservoir below the permissible salinity level. This study showed that this could be accomplished mainly by controlling the salinity at the pumping wells and the size of the residual saltwater mass in the reservoir. For this reason, observation equipment for measuring the salinity of the pumped water is installed at each pumping well and the data are monitored at a central management facility. The size of the residual saltwater mass is checked using observation wells.

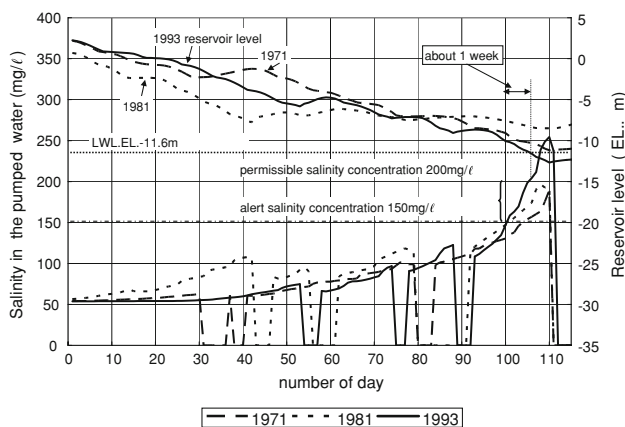## Management of the salinity of the pumped water

To keep the salinity of irrigation water under the permissible salinity level, it is necessary to manage the water quality of the pumped water carefully by establishing an index value that shows whether the saltwater concentration is likely to be more than the permissible value. Therefore, saltwater intrusion was analyzed for the design reference year 1971, for drought years (7 years, including 1981) in which conditions were the same as in the reference year, and for a drought year 1993 in which conditions exceeded those of the design reference year. The following points are noteworthy.

The alert salinity level

Figure 15 shows elapsed days and the increase in the salinity of the pumped water in relation to the reservoir level for each year. When the salinity of the pumped groundwater is found to be more than 150 mg/l, it is likely that it will exceed the permissible value about 1 week later. Therefore, 150 mg/l of chlorine was set as the alert salinity level. When this level of salinity is observed, it is necessary to take appropriate measure to keep the salinity from exceeding the permissible level (200 mg/l of chlorine).

The alert reservoir level

The reservoir level is gradually lowered as water is used for irrigation. The salinity reaches the alert salinity level when the reservoir level is –10 m, which is considered the alert reservoir level. Moreover, when the reservoir level drops below –11.6 m, the likelihood that the salinity will exceed the permissible value is high. Therefore, it is necessary to keep the water level above this water level by restricting water pumping when it approaches this level.

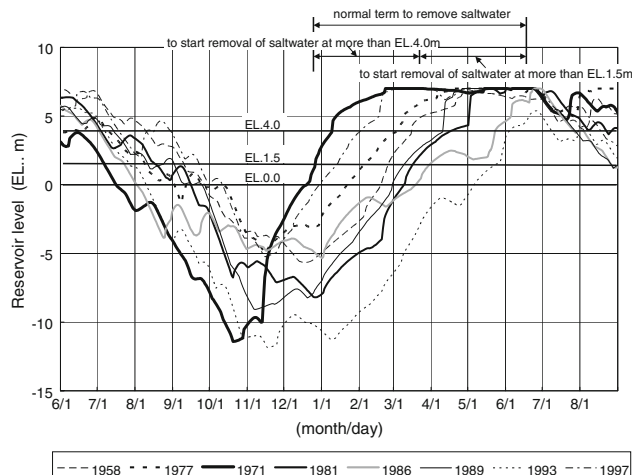## Management of the residual saltwater mass

In drought years, saltwater intrusion due to the reduced reservoir level increases the saltwater mass, causing the level of the saltwater–freshwater interface to occasionally exceed the target management level of the saltwater–freshwater interface. In the year following a dry year, saltwater should be removed from the residual saltwater mass to reduce the level of the saltwater–freshwater interface to the management level.

The saltwater should be removed after the reservoir level recovers, from January to June of the year following the year in which the reservoir level becomes low (Fig. 16). The saltwater is removed most efficiently when water overflows from the dam, because then the saltwater tends to move toward the cutoff wall (Fig. 10). Therefore, the saltwater should be removed from January to March, after confirming that the reservoir level is more than 4 m and the dam is overflowing, before full-scale irrigation begins. When the reservoir level is above 1.5 m, the saltwater should be removed from April to June.

For salinity management, this project is equipped with each of the three wells (pumping capacity per well, 2,000–2,500 m^3/day) to remove the saltwater in the residual saltwater area in the western and eastern part and to reduce the level of the saltwater–freshwater interface to each target management level.

Conclusions

The Komesu underground dam is the first full-scale underground dam constructed to prevent saltwater intrusion in Japan. Although the cutoff wall of the dam effectively reduces the movement of saltwater into the reservoir area,

Fig. 15 Salinity in the pumped water and number of days in the reservoir level downturn (W section, No. 3 well). Note: When the salinity is 0, driving of the pump stops

Fig. 16 Variation of simulated reservoir level and time of saltwater removal in drought years

saltwater masses remained behind the dam at the time of its completion, and saltwater can intrude beneath and diffuse through the wall, particularly when the reservoir level is below the sea level because of the high pumping levels during the drought years. Therefore, it is necessary to estimate in advance whether the salinity in the pumped water is likely to exceed the permissible salinity level because of an increase in the residual saltwater mass as a result of saltwater intrusion.

To analyze saltwater intrusion, we selected the optimal program suitable for the analysis of saltwater intrusion into the Komesu underground dam, using the result of the two-dimensional residual saltwater movement analysis on inclined ground and recreating the movement of residual saltwater in the water tank experiment. The longitudinal dispersivity parameter of the convective–dispersive equation must be determined before the analysis of saltwater intrusion can be carried out. Through successful results of the longitudinal dispersivity parameter on limestone have not been obtained in Japan, we attempted a tracer experiment and obtained it around the pumping wells.

Based on these results, we analyzed saltwater intrusion into the reservoir area in detail by using a two-dimensional convective–dispersive analysis. This result showed that the well groups near the residual saltwater masses were affected by both residual and intruded saltwater when water was pumped in the simulation based on the design reference year and the salinity was higher than the permissible salinity level. Therefore, we estimated the target management level of the saltwater–freshwater interface. The salinity of the pumped water in the design reference year would be lower than the permissible salinity level if saltwater is removed before every full-scale irrigation period to reduce the level of the saltwater–freshwater interface to the target management level.

In this project, we were equipped to take the necessary measures for each of the three wells to remove the saltwater in the residual saltwater area in the western and eastern part. The actual levels of the saltwater–freshwater interface in each case were reduced to the target management level, and the water quality management manual for salinity in the reservoir area of the Komesu underground dam was formulated.

This study is based on the numerical calculation based on two-dimensional convective–dispersive analysis. It is necessary that the application of this analysis should be examined on the basis of data, which will be observed by the management facility. Depending on these results, necessary measures should be taken to manage water quality for salinity more suitably in the reservoir.

References

Boufadel M, Suidan M, Venosa A (1999) A numerical model for density-and-viscosity-dependent flows in two-dimensional variable saturated porous media. J Contam Hydrol 37:1–20

Guo WG, Langevin CD (2002) User's guide to SEAWAT: a computer program for simulation of three-dimensional variable-density ground-water flow. US Geological Survey Techniques of Water-Resources Investigations 6-A7:77

Henry H (1959) Salt intrusion into fresh-water aquifers. J Geophys Res 64:11

Momii K, Hosokawa T, Kono K, Itoh T (1989) Estimation method of transverse dispersivity based on vertical salt concentration distribution in coastal aquifer. In: Proceedings of Japan Society of Civil Engineers, vol 411(II)-12, pp 45–53 (in Japanese)

Nawa N, Nakao J, Miyazaki K, Muramami G (2008) The analysis method of salt water intrusion and the field test for dispersion paramerters in Komesu underground dam. J Jpn Soc Irrigation Drainage Rural Eng 76-1:21–24 (in Japanese)

NIPOOMISAD (The National Irrigation Project Office of The Okinawa Main Island Southern Area District) (2006) Engineering journal-national irrigation project at Okinawa Main Island southern district, pp 133–152 (in Japanese)

Nishigaki M, Hishiya T, Hashimoto M, Kouno I (1995) The numerical method for saturated–unsaturated fluid density-dependent groundwater flow with mass transport. In: Proceedings of Japan Society of Civil Engineers, vol 511(III)-30, pp 135–144 (in Japanese)

Nishigaki M, Mitsubishi Materials Corp, Daiya Consultant Corp (2001) Density-dependent transport analysis. Saturated–unsaturated porous media: 3-dimensional Eulerian Lagrangian method (in Japanese)

Sauty JP (1989) An analysis of hydrodispersive transfer in aquifer. Water Resour Res 16(1):145–158

SES (Soil Engineering Society) (2002) Survey, estimation and measure of soil and groundwater pollution, Hokosha Publication, pp 107 (in Japanese)

SGGP (Study Group of Groundwater Problem) (1991) Pollution theory of groundwater: foundation and application. Kyoritu Publication, pp 197–208 (in Japanese)

Voss CI, Provost AM (2003) SUTRA: a model for saturated–unsaturated, variable-density groundwater flow with solute or energy transport, U.S. Geological Survey Water-Resources Investigations Report 02-4231, pp 250